MATHEMATICAL BIOSCIENCES
AND ENGINEERING
Volume **7**, Number **4**, October **2010**

doi:10.3934/mbe.2010.7.793

pp. **793–807**

MINIMAL STATE MODELS FOR IONIC CHANNELS INVOLVED IN GLUCAGON SECRETION

Virginia González-Vélez

Dept. Ciencias Básicas, Universidad Autónoma Metropolitana Azcapotzalco
México D.F., 02200, Mexico

Amparo Gil

Dept. Matemática Aplicada y Ciencias de la Computación, Universidad de Cantabria
Santander, 39005, Spain

Iván Quesada

Instituto de Bioingeniería, Universidad Miguel Hernández
Elche, 03202, Spain

(Communicated by Yang Kuang)

Abstract. Pancreatic alpha cells synthesize and release glucagon. This hormone along with insulin, preserves blood glucose levels within a physiological range. During low glucose levels, alpha cells exhibit electrical activity related to glucagon secretion. In this paper, we introduce minimal state models for those ionic channels involved in this electrical activity in mice alpha cells. For estimation of model parameters, we use Monte Carlo algorithms to fit steady-state channel currents. Then, we simulate dynamic ionic currents following experimental protocols. Our aims are 1) To understand the individual ionic channel functioning and modulation that could affect glucagon secretion, and 2) To simulate ionic currents actually measured in voltage-clamp alpha-cell experiments in mice. Our estimations indicate that alpha cells are highly permeable to sodium and potassium which mainly manage action potentials. We have also found that our estimated N-type calcium channel population and density in alpha cells is in good agreement to those reported for L-type calcium channels in beta cells. This finding is strongly relevant since both, L-type and N-type calcium channels, play a main role in insulin and glucagon secretion, respectively.

1. **Introduction.** The pancreas is the organ in vertebrates that produces glucagon, insulin and somatostatin hormones through its exocytotic cells α, β and δ, respectively. These cells are grouped in areas called Islets of Langerhans. Each islet is made up of 1000 to 3000 cells, of which alpha cells represent 33 to 46% in humans, and 15 to 20% in mice [5]. Thus, a mouse islet only has between 150 and 600 alpha cells. Because of the scarcity of α-cells in the mouse islet and the difficulties in identifying them according to physiological patterns, the information about this cell type is limited in comparison to the β-cell. Alpha cells synthesise and release glucagon. This hormone along with insulin, preserves blood glucose levels within a physiological range. Glucagon is secreted during hypoglycemia, and in turn, it induces the

2000 *Mathematics Subject Classification.* Primary: 92B05; Secondary: 92C30.
Key words and phrases. Markov models, pancreatic alpha cell, ionic channels, Monte Carlo.

mobilisation of hepatic glucose into the bloodstream. In diabetic individuals, the α-cell function may be impaired, which can aggravate the hyperglycaemic state of these patients. Because of its vital role in glucose regulation, understanding alpha cell physiology is a key topic in the treatment of diabetes [24].

From a physiological point of view, the electrical activity exhibited by alpha cells is initiated when they are exposed to low glucose levels. In this situation, the alpha cells generate action potentials (APs) which are related to glucagon secretion. These APs are supposed to be triggered by a low ATP/ADP ratio, because of the absence of glucose. In these conditions, the K_{ATP} channels are open, producing an ionic current that allows a level of membrane potential where APs are generated. This electrical activity chain is possible thanks to the Ca^{2+} and Na^{+} channels that fire the depolarisation stage of the APs. Then, cell depolarisation finally activates the K^{+} channels in order to repolarise the cell [24, 14]. Some experimental studies vary the glucose level to explore regulating factors of glucagon secretion [34]. Other experiments focus on the electrical activity involved in glucagon secretion [13, 2, 12]; a common protocol in these works is to stimulate the cell with controlled depolarising pulses from a fixed cell voltage, and then measure the produced ionic currents (voltage-clamp technique).

In this paper, we define minimal state models and estimate their parameters for each ionic channel, towards simulating ionic currents associated to glucagon secretion in alpha cells. Currently, we are only considering the relevant currents measured in mice, which are common animal models for alpha-cell experimentation. We present a state modeling approach to simulate the dynamics of ionic currents commonly measured in voltage-clamp experiments on alpha cells. Among other findings, we have noticed that our N-type calcium channel density in alpha cells is in the order of the L-type channel density reported for beta cells [3], which is interesting since both channels are involved in glucagon and insulin secretion, respectively.

2. **Physiological basis.**

As in many cell types, glucagon release is regulated by intracellular Ca^{2+} increases which in turn involve voltage-gated Ca^{2+} channels. Even though Ca^{2+} plays a main role in alpha-cell exocytosis, other voltage-gated ionic channels are also involved in the electrical activity leading to glucagon secretion, including Na^{+} and K^{+} channels [14]. The main alpha-cell electrical currents associated to glucagon secretion are the T- and N-type calcium currents (I_{Ca_T} and I_{Ca_N}), the sodium current (I_{Na}) and the DR- and A- type potassium currents ($I_{K_{DR}}$ and I_{K_A}) [24]. These are all voltage-dependent currents due to the activation of specific ionic channels. Although there are other currents found in α-cells, such as the L-type calcium current and the ATP-regulated potassium current, they are not being included as we are focusing on the main voltage-dependent electrical currents directly involved in glucagon release. The L- calcium current is voltage-dependent and contributes to calcium influx, but it hardly participates in glucagon exocytosis in response to glucose [14]. The ATP-dependent current, on the other hand, is not voltage-dependent since it is controlled by the glucose metabolism. In this paper, we will consider that glucose remains constant at a physiological value (5 mM), which is a common condition in depolarisation-evoked experiments.

Voltage-dependent electrical currents that control the sequence of events leading to glucagon secretion, that is I_{Ca_T}, I_{Ca_N}, I_{Na}, I_{K_A} and $I_{K_{DR}}$, exhibit some common kinetic properties that make them suitable for modeling. First, the activation of

these currents increases as the cell membrane changes its potential difference between the inside and the outside of the cell, i.e. as the cell becomes depolarised. Second, the currents deactivate when depolarisation disappears. Third, a strong or a sustained depolarisation induces current inactivation (in some of these currents) i.e. the current diminishes even when depolarisation continues. However, each current exhibits its own dynamic behaviour. Hence, these properties serve as a basis for state models since these channels produce the whole-cell currents measured during electrophysiological experiments on alpha cells.

3. **Minimal models.** There are two common approaches to model channel gating that produce ionic currents: the Hodgkin-Huxley paradigm and the Markov state modeling [8]. The first is widespread because of its capability to be managed and its ability to model macroscopic phenomenon so, there are different parameter estimation methods and software based on it [40, 39]. However, this approach is unable to model single-channel behaviour since it is based on continuous and deterministic principles [6, 31, 15]. Markov state models are an adequate methodology to combine experimental information and mathematical modeling of single-channel behaviour [23] since each state is trying to resemble the conformational changes suffered by the channel, in order to reproduce whole-cell measurements. In this paper we develop Markov state models for channels towards: 1) Understanding individual alpha-cell ionic channel functioning and modulation that could affect glucagon secretion, and 2) Simulating ionic currents actually measured in voltage-clamp alpha-cell experiments. These channel models are suitable to be incorporated in microscopic schemes capable to simulate high-resolution temporal and spatial events related to glucagon exocytosis, as done in other cell types [10, 37].

Based on the idea that transition rates could be interpreted as transition probabilities per time unit, we propose one state model for each ionic channel and associate each transition rate between states (q_{ij}) to a channel property (Figure 1). A model contains just one Open (and active) state and one or more Closed and Inactive states; the Open (active) is the conducting state. Specifically, we understand *Activation* as those transitions going to the Open state, and *Deactivation* as those transitions going to Closed states. Activation and deactivation are both functions of membrane voltage in a symmetrical manner. Since some channels also present *Inactivation* (no response under constant stimulation), we understand it as transitions to Inactive states. There are two types of channel inactivation: due to extreme depolarisation (voltage-dependent inactivation), and due to the accumulation of Ca^{2+} near the channel mouth (calcium-dependent inactivation) [41]. Our models have both cases and the dependence is included in the definition of the transition rate to Inactive states. All transition rates follow the main idea of the Markov models, i.e. transitions only depend on the present state and are time-independent [6, 25]. The minimal models proposed here are constrained to fit an experimental current-to-voltage (IV) function and to adequately reproduce dynamic currents; as possible, we also take into account other kinetic data such as steady-state inactivation curves or time constants. Our models are based on previously reported models where possible, but are simplified in order to have the minimum number of states to reproduce current dynamics and to uncover intrinsic channel properties.

Following the idea that activation/deactivation are symmetrical exponential functions of membrane potential difference [8], we define opening and closing rates as

(a)

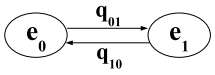

$$\frac{dP_{e_0}}{dt} = q_{10}P_{e_1} - q_{01}P_{e_0},$$
$$\frac{dP_{e_1}}{dt} = q_{01}P_{e_0} - q_{10}P_{e_1}.$$

(b)

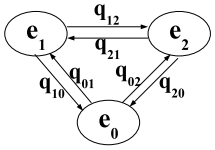

$$\frac{dP_{e_0}}{dt} = (q_{10}P_{e_1} + q_{20}P_{e_2}) - (q_{01} + q_{02})P_{e_0},$$
$$\frac{dP_{e_1}}{dt} = (q_{01}P_{e_0} + q_{21}P_{e_2}) - (q_{10} + q_{12})P_{e_1},$$
$$\frac{dP_{e_2}}{dt} = (q_{02}P_{e_0} + q_{12}P_{e_1}) - (q_{20} + q_{21})P_{e_2}.$$

(c)

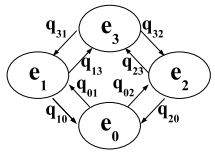

$$\frac{dP_{e_0}}{dt} = (q_{10}P_{e_1} + q_{20}P_{e_2}) - (q_{01} + q_{02})P_{e_0},$$
$$\frac{dP_{e_1}}{dt} = (q_{01}P_{e_0} + q_{31}P_{e_3}) - (q_{10} + q_{13})P_{e_1},$$
$$\frac{dP_{e_2}}{dt} = (q_{02}P_{e_0} + q_{32}P_{e_3}) - (q_{20} + q_{23})P_{e_2},$$
$$\frac{dP_{e_3}}{dt} = (q_{13}P_{e_1} + q_{23}P_{e_2}) - (q_{31} + q_{32})P_{e_3}.$$

FIGURE 1. State models for all channels. (a) Two-state model for potassium channels associated to $I_{K_{DR}}$. e_0 and e_1 represent *Open* and *Closed* channel states, respectively. (b) Three-state model for both types of calcium channels (I_{Ca_T} and I_{Ca_N}). e_0, e_1, e_2 correspond to *Open*, *Closed* and *Inactive* states, respectively. (c) Four-state model for sodium and potassium channels associated to I_{Na} and I_{K_A} currents. e_0, e_1, e_2, e_3 correspond to *Open but Inactive*, *Closed and Inactive*, *Open*, and *Closed* states, respectively. The values for all of the transition rates are given in Table 2. The system of differential equations corresponding to each model is shown in the right.

exponential functions. Inactivation rates are defined as sigmoidal functions of membrane potential difference, considering that experimental data commonly shows that currents inactivate in this manner. For the N-type Ca^{2+} channels, we also added calcium-dependent inactivation since these channels exhibit this particularity, as discussed in [16]. Finally, all other transition rates are fitted as time constants, as is the case in many state models. All models include one Open and some Closed and Inactive states, depending on the specific channel characteristics, as depicted in figure 1. Although there are other methods to estimate current kinetic properties [33] using the Hodgkin-Huxley approach, we favour the voltage-clamp experimental basis to estimate model parameters.

4. **Parameter estimation.** Parameter estimation for each model was done using a Monte Carlo algorithm which looks for a parameter set that fits an experimental IV curve with minimal error. If there is information about an experimental IV relationship in alpha cells, we have used it to calibrate our model. However, since some currents have not yet been isolated or measured in alpha cells, we have

used data available from experiments on other cell types considering that channels preserve their single-channel properties. Although we are not following a formal methodology to fit kinetic parameters since there is no available numerical data for single or total currents, our algorithm considers the guidelines discussed in [22]: 1) To fit the model several times while randomly changing the parameters; 2)To fix some parameters to improve the identifiability of the model; 3)To make the number of trials large enough (proportional to parameter space) to improve confidence, and 4)To use a defined stimulation (like a depolarising pulse). Our main algorithm is shown in Figure 2: First, it determines the number of trials as a function of the number of parameters; then, it generates random parameter combinations for the parameter space (routine randPar(numPar)); after, it calculates the peak current at specific voltages by solving channel equations for each parameter set (routine channel(V,p)); finally, it computes the chi square deviation of the simulated peak currents to experimental ones, and find that set with minimal deviation (routine minChiDev()).

Routine channel(V,p) solves the system of differential equations representing each channel model (Figure 1), at the steady state. Specifically, it obtains the peak current for each model at the specific voltage V with the parameter set p. For example, for the two-state model (Figure 1(a)), the equations are

$$\begin{aligned} P'_{e_0} &= q_{10}P_{e_1} - q_{01}P_{e_0}, \\ P'_{e_1} &= q_{01}P_{e_0} - q_{10}P_{e_1}, \end{aligned} \tag{1}$$

where P_{e_i} represents the probability that a channel is in state e_i. An extra equation refers to probability conservation i.e. $\sum_n P_{e_n} = 1$. The solution to (Eq.1) for P_{e_0} and P_{e_1} at the steady-state (i.e. where each $P'_{e_i} = 0$), would be

$$\begin{aligned} P_{e_0} &= \tfrac{q_{10}}{q_{01}+q_{10}}, \\ P_{e_1} &= \tfrac{q_{01}}{q_{01}+q_{10}}, \end{aligned} \tag{2}$$

which has two rates to be fitted, q_{10} and q_{01}. For this two-state model, these transition rates refer to the activation and deactivation of the channel, and as mentioned above, they are exponential functions of the membrane potential. Indeed, there are two parameters per exponential to be fitted (amplitude and time constant) so, for the two-state model the parameter space is made of five parameters in total: four for the rates, and one for the channel population. It is important to mention that the number of channels is always considered to be a free parameter ranging between 100 and 10000; these limits are based on density values for beta and chromaffin cells [21, 17] (see Section 6 for a broader discussion about channel densities). Routine randPar(numPar) generates the random values for all parameters for each trial, considering these limits.

The solution for the Open state probability (P_{e_0} in Eq.(2)) allows estimation of the number of open channels. The total current is calculated multiplying the unitary current by the open channel population, as described for L- calcium channels in [11]. The unitary current is specific to each channel, and it depends on the membrane voltage and the single-channel conductance; these values are given in Table 1 for all channels. The fixed values used to estimate the free parameters and to simulate the electrical currents, are detailed in Table 1. The estimated values for the transition rates for each channel model, are given in Table 2. The physiological basis for each channel model and its associated ionic current are detailed in section 5.

```
INPUT(numPar)
OUTPUT(best)
begin N = 1,000,000 * numPar
  for j := 1 to N do
      p(j) = randPar(numPar);
      for V := V_low to V_hi do
          I(j) = channel(V, p(j));
      end
  end
  for j := 1 to N do
      best = minChiDev(I(j), Iexp));
  end
end
```

FIGURE 2. Algorithm used to find the best parameter set that fits experimental peak currents for each channel model.

TABLE 1. Fixed values for channel models

	Ca_T	Ca_N	Na	K_A	K_{DR}
Unitary conductance (pS)	8.4,4.2,2†	13	12,4‡	12	30
Activation voltage, V_{act} (mV)	-60	-20	-30	-40	-20
Inactivation voltage, V_{in} (mV)	-45	-31	-42	-68	—

†4.2pS if $V > -60$, 8.4pS if $V \leq -60$, 2pS if $V > 0$. See also section 5.4.
‡12pS if $V \leq 10$, otherwise 4pS. See also section 5.3.

4.1. **Dynamic behaviour vs. steady-state estimation.** Using an optimal set of parameters for each model, we simulate the dynamic behaviour of a current by solving the differential equations over time for each multi-state model. We try, in this manner, to reproduce the measured currents following experimental protocols in alpha cells. These protocols usually consist of fixing a resting condition for the cell (at a very negative membrane potential), and then stimulating it by depolarising the cell membrane. For our simulations, all channels are assumed to be closed at resting (initial) conditions, and they increment their opening probability as depolarisation increases. We again compute the total current as the product of the number of channels in the Open state by the unitary current, per each time step. The algorithm uses an adaptive time-step ordinary differential equation solver for stiff problems (*ode15s*) implemented in Matlab (http://www.mathworks.com).

It is important to mention that there is a strong compromise between fitting an IV curve, and correctly reproducing the current dynamic behaviour. On the one hand, the IV curve is built from peak currents (as in experimental reports) which corresponds to the maximal conductance of a channel population, i.e. the maximum number of channels that could be open due to the electrostatic force of the applied membrane potential difference. This is calculated on the basis that Open probability rapidly increases for membrane depolarisations, so peak current value is mainly due to steady-state Open probability. On the other hand, the

TABLE 2. Estimated values for channel models. All rates in ms^{-1}.

	Sodium	A-type potassium
NC	2554	1631
q_{01}	$0.44\exp(-0.06V_{th})$	$6.83\exp(-0.02V_{th})$
q_{10}	$11.39\exp(0.05V_{th})$	$30.77\exp(0.03V_{th})$*
q_{02}	0.81*	$8.5\,10^{-5}$
q_{20}	$9.06/E_0$	$0.01/E_0$*
q_{13}	0.004*	0.008
q_{31}	$3.69/E_0$*	$0.12/E_0$*
q_{23}	$0.8\exp(-0.06V_{th})$	$0.8\exp(-0.02V_{th})$
q_{32}	$20.58\exp(0.05V_{th})$	$3.6\exp(0.03V_{th})$*

	T-type calcium	N-type calcium	DR-type potassium
NC	694	202	251
q_{01}	$0.03\exp(-0.05V_{th})$	$0.22\exp(-0.05V_{th})$	$2.6\,10^{-5}\exp(-0.2V_{th})$
q_{10}	$13.06\exp(0.03V_{th})$	$0.67\exp(0.04V_{th})$	$0.7\exp(0.03V_{th})$
q_{02}	0.001	–	–
q_{20}	$8.94/E_1$	–	–
q_{12}	$89.4/E_1$	$6.9(\Delta Ca/E_1)$*	–
q_{21}	0.001	0.008*	–

NC=Number of channels, $V_{th} = V - V_{act}$, $V_i = V - V_{in}$.
$\Delta Ca = \frac{[Ca]_i}{[Ca]_o}$, $E_0 = 1 + \exp(-0.01V_i)$, $E_1 = 1 + \exp(-0.1V_i)$.
*Values modified to improve dynamic behaviour. See section 4.1 for details.

dynamic behaviour of the current exhibits the rapid and transitory changes of the channel, i.e. the transitions to/from one state to another, including the Open state. This is attributable not only to membrane potential variations but also to stochastic transitions over time. Using this approach, the set of parameters found for peak currents is a static approximation of this behaviour, and does not necessarily reproduce current dynamics although it provides a good set of starting values to restrict the model and the channel populations.

To overcome this limitation and bearing in mind that our main goal is to study the real electrical activity observed in alpha cells, we have taken the channel model parameter set obtained while fitting the IV curve, as described above, as a starting set of parameters to simulate the corresponding current dynamics. After the simulations, we observed that some dynamic properties, mainly deactivation and inactivation, were underestimated. We tested different options in order to simulate experimental currents. The most suitable was to fix deactivation parameters and to increase inactivation amplitudes. Then we checked that the new IV curve was not far off the expected values, considering the reported experimental error bars. This method has been applied to the channel models for I_{Na}, $I_{K_A}$and I_{Ca_N}. Figure 3 shows an example of this methodology for I_{Na}, where comparisons between the IV curves, and the underestimated vs. modified currents are demonstrated. The final IV curves obtained for all channel models using parameters given in Table 2, are shown in Figure 4. Modified parameters are marked in this table with an asterisk.

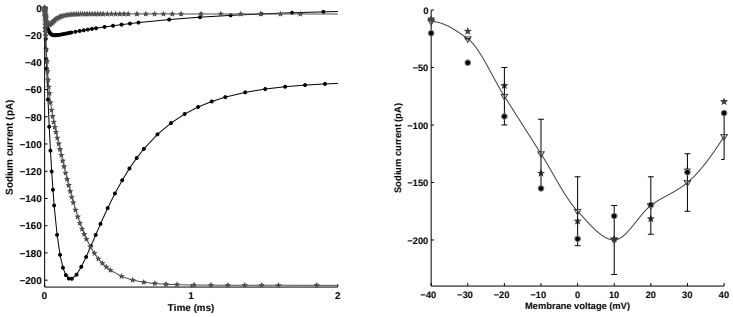

(a) (b)

FIGURE 3. Example of the limitations of static parameter estimations to adequately reproduce dynamic behaviour. (a) Comparison of sodium currents induced by two depolarisations: strong (0 mV, large currents) and weak (-40 mV, small currents). Currents were simulated using: 1)The static parameter set obtained by fitting the IV curve (stars), and 2)The modified set (dots). As observed, parameter modifications improve dynamic simulations; in this case, new parameter values allow fast sodium current inactivation as found in alpha-cell experiments [2]. (b) Comparison of IV curves: experimental read from [2] (triangles, error bars and line), static best-fit (stars) and modified (dots). Notice that parameter modifications do not significantly affect the IV curve fitting since new values still fall inside experimental error bars.

5. **Simulated currents from channel models.** Following we discuss the available experimental data for each ionic channel and current, and how this information has been used to define a particular channel model. Once a channel model has a fixed set of parameters, we test the performance of the model in two ways: simulating the IV curve and the ionic current over time.

5.1. **A-type K^+ channels.** We have considered two voltage-dependent potassium currents in this work: the $I_{K_{DR}}$ and the I_{K_A}. These currents are named "outward currents" since channels allow K^+ to go out of the cell when they are open, in contrast to calcium and sodium currents which are named "inward currents". I_{K_A} is due to $K_V4.3$ channels, a voltage-gated potassium channel type which is present in alpha cells, neurons and myocytes. In all these cell types, I_{K_A} plays a very important role since it regulates membrane potential and it initiates repolarisation after action potentials [1, 24]. Some sophisticated models simulate $K_V4.3$ channel behaviour in other cell types (not alpha cells) (see for example [38]). In all of these models there are several Closed states, one Open state and several Inactive states, including Open-Inactive and Closed-Inactive states. Because of its kinetics, it resembles voltage-gated sodium currents: activates at negative membrane potentials, presents a sustained steady-state current and shows voltage-dependent rapid inactivation. In accordance, we propose a four-state minimal model for I_{K_A} (see figure 3).

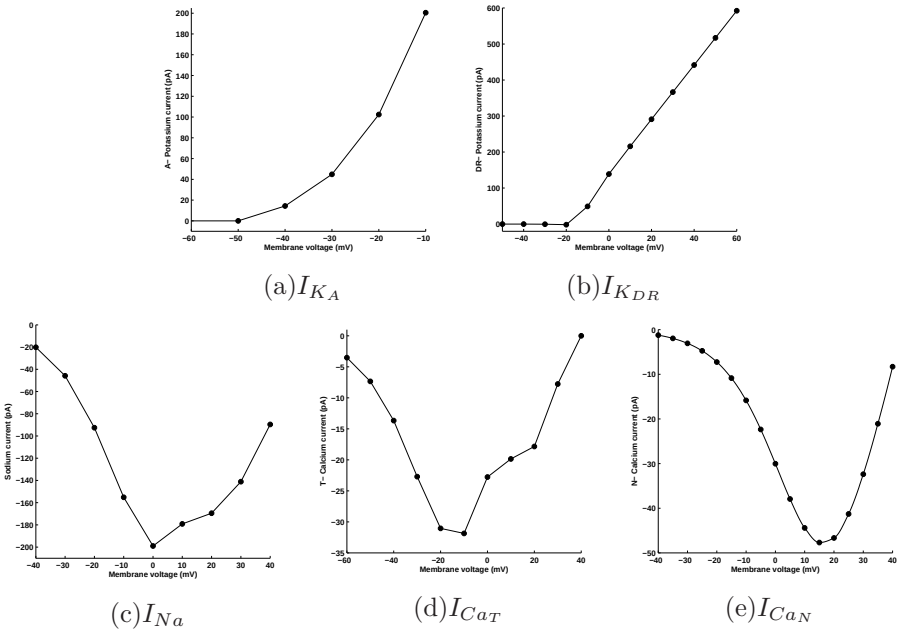

(a)I_{K_A} (b)$I_{K_{DR}}$

(c)I_{Na} (d)I_{Ca_T} (e)I_{Ca_N}

FIGURE 4. Simulated current-to-voltage (IV) curves for all channel models, using the parameter values given in Tables 1 and 2.

In alpha cells, I_{K_A} activates above -50 to -40 mV and exponentially increases with depolarisation. It exhibits voltage-dependent inactivation with half-maximum point at -68 mV [12]. In other cell types (not α-cells) unitary conductance of $K_V4.3$ channels has been established between 12 to 19 pS, for asymmetrical internal and external K^+ concentrations [1], so we assume a value of 12 pS for our simulations since alpha cells are commonly exposed to asymmetrical K^+ quantities. In Figure 5(a) we show the simulated I_{K_A} currents obtained for the activation and deactivation voltages proposed by [12], and with the parameters given in Table 2.

5.2. **DR-type K^+ channels.** $I_{K_{DR}}$ is produced by $K_V2.1$ channels which are potassium channels managed by voltage; these channels are found both in alpha and beta cells [14]. In beta cells, the activation threshold has been found at -20 mV and its IV curve shows that current grows as depolarisation increases [32]. This current does not exhibit any inactivation so we propose a minimal two-state (Open-Close) model, as shown in Figure 3. The unitary conductance of $K_V2.1$ channels has been estimated in 30.1±8.0 pS for neural stem cells [30]. Figure 5(b) shows the simulated $I_{K_{DR}}$ currents produced with the two-state model and the parameters given in Tables 1 and 2.

5.3. **Na^+ channels.** Na^+ channels are completely voltage driven, and they have been modelled with many Closed and Inactive states in addition to one Open state, such that the channel may inactivate from the Open or the Closed states [35]. Our minimal model then includes four states: one Closed, one Open and two Inactive states, as shown in Figure 1. Sodium channels activate and inactivate as a function of membrane potential with a threshold voltage in the range of -30 to -20 mV [12, 2, 36]. Single channel properties of these channels have not been estimated in

α-cells. In Purkinje cells, a unitary conductance of 12 pS using 140 mM of external sodium concentration, as well as a channel population of 167 channels per square micron, have been estimated [28]. In squid axon, unitary conductance was estimated as 14 pS, with a channel population of 180 per square micron [35]. In alpha cells, an activation voltage of -30 mV has been reported as well as a half-maximal inactivation voltage of -42 mV [2]. This work also reports that approximately 200 pA are obtained for a depolarisation of -70 to 0 mV, although a much larger current (about -545 pA) has been reported in other work [12]. Over this basis, we take a unitary conductance of 12pS for voltages less than 10 mV, and 4 pS for greater voltages. Activation and inactivation voltages are taken from [2]. Estimated parameters are given in Table 2. In Figure 5(c) we show simulated I_{Na}currents with these values taking into account that the model should reproduce the fast activation-deactivation kinetics in a time scale below 5 ms, as observed in alpha-cell experiments [2, 12].

5.4. **T-type Ca^{2+} channels.** Two types of Ca^{2+} channels are considered: the T- and the N-. The T-type channels have been modelled as having one Open and many Inactive and Closed states, with possible transitions from/to Inactive to/from Open and Closed states [27]. So, a model should include Closed, Open and Inactive states, and should take into account that the channel may inactivate from the Open and the Closed states. Since these channels exhibit Open-state and Closed-state inactivation, and considering that both inactive states reach a fast equilibrium [27], we are proposing a minimal 3-state model (Figure 1b) for which transitions to the Inactive state from the Open or the Closed states are similar.

There are two different experimental observations for T- currents in alpha cells concerning activation voltage: -40 mV [12, 18, 19] and -60 mV [18, 19]. Considering these experimental works and in order to define the parameters of our model, we are assuming that T-type calcium channels activate above -60 mV (in agreement with the proposed role of pacemakers for T- channels [24, 41]), and that the peak current ($\sim$27 pA) is reached at -20 mV . We are taking the unitary conductances reported for neurons: 4.2 pS for voltages above -60 mV (broader range), 8.4 pS below -60 mV, and 2 pS for positive voltages to obtain small currents [4].

It is well worth noticing that modeling inactivation for T- channels is not easy since inactivation and recovery could bypass the Open state [27]. In alpha cells, the $I_{Ca_T}$is transient, fast activated and seems to be rapidly inactivated in a voltage-dependent manner [19]. Moreover, T- currents exhibit an overcrossing behaviour over depolarisation [4], so peak currents do not follow the hierarchy of steady-state currents. Thus, to estimate parameters for the T- channel model we used a routine channel that calculates dynamic solutions instead of steady-state values, considering a half maximal inactivation at -45mV [12]. Deactivation has to be fixed to achieve a transient behaviour in the first few milliseconds. Figure 5(d) shows the resultant I_{Ca_T}currents obtained with the parameters shown in Table 2.

5.5. **N-type Ca^{2+} channels.** N-type calcium channels do not exhibit transitions from the Open to the Inactive state, and they exhibit some calcium inactivation [16]. Hence, we propose a minimal model with Open, Closed and Inactive states with possible transitions only from the Open to the Closed and from the Inactive to the Closed, and viceversa, i.e. transitions q_{02} and q_{20} are zero. An important dependence included in the inactivation rate is $\Delta Ca = Ca_o/Ca_i$, which estimates the increase in the internal calcium concentration ($[Ca^{2+}]_i$) compared to the external concentration ($[Ca^{2+}]_o$). In this calculation we are assuming that $[Ca^{2+}]_o$ remains

constant at 2.5mM, which is reasonable since the external medium is four orders of magnitude greater than the internal concentration (Basal $[Ca^{2+}]_i \sim 0.1\mu M$), and that $[Ca^{2+}]_i$ is varying each time step. This is done assuming local diffusion along 100 nm from the cell membrane without buffering. We have made some tests with buffered diffusion and the results have shown that inactivation only varies by a constant factor. So, it is valid to use our approximation to estimate an upper limit for calcium-dependent inactivation.

I_{Ca_N} activates between -40 and -20 mV [24, 16]. Single-channel data has been measured in neurons (where unitary conductance is between 13 to 15 pS [16]) and in embryonic kidney cell lines (where unitary conductance is 12 pS [9]). In alpha cells, the N- current represents about one third of the total calcium current (the rest is L- and T- current), and it has been estimated in ∼50 pA when the cell becomes depolarised from -70 to +10 mV [20]. In this paper, the activation and inactivation voltage have been estimated in -20 mV and -31 mV, respectively, so we take them as fixed values for the model, as well as 13 pS of unitary conductance. Simulated I_{Ca_N} currents, obtained with the parameters given in Table 2, are shown in Figure 5(e).

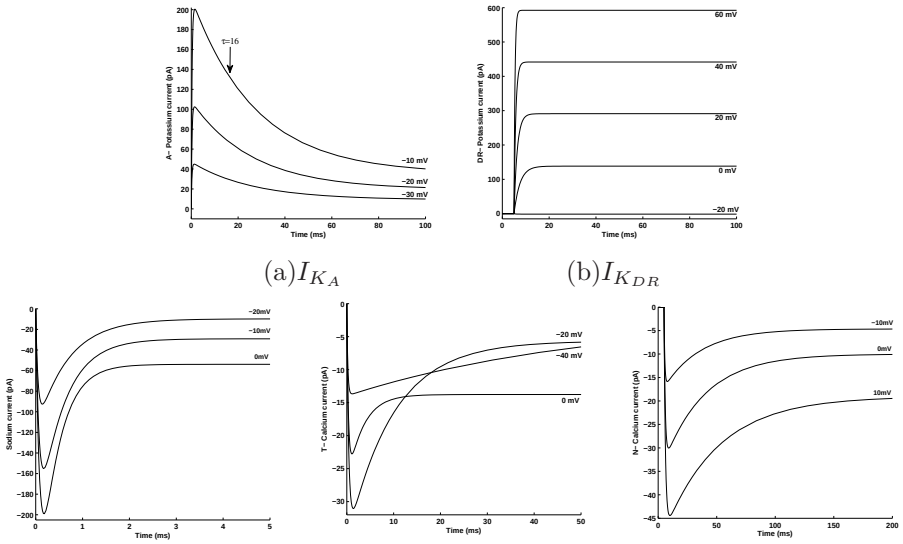

(a)I_{K_A} (b)$I_{K_{DR}}$

(c)I_{Na} (d)I_{Ca_T} (e)I_{Ca_N}

FIGURE 5. Simulated dynamic currents following the experimental protocols reported in the references. Notice differences in time scales. (a) A-type potassium currents for -30, -20 and -10 mV. The arrow over the largest current indicates the value of our time constant ($\tau = 16ms$) which is in agreement with experimental findings [12]. (b) DR-type potassium currents for -20 to +60 mV [32]. (c) Sodium currents for -20, -10 and 0 mV [2]. (d) T-type calcium currents obtained for -40, -20 and 0 mV [19]. Notice the currents overcrossing, as observed in experiments [4]. (e) N-type calcium currents for -10, 0 and 10 mV [20].

TABLE 3. Estimated conductances and densities in alpha cells

	Ca_T	Ca_N	Na	K_A	K_{DR}
Estimated number of channels	694	202	2554	1631	251
Single-channel conductance (pS)	4.2	13	12	12	30
Max. whole-cell conductance (nS)	2.9	2.6	30.6	19.5	7.5
Density† (channels per μm^2)	2.2	**0.6**	8.1	5.2	0.8

†Considering a spherical alpha cell, radius=5 μm

6. **Discussion.** The ionic currents simulated in this paper are based on minimal state models for those ionic channels related to glucagon secretion in pancreatic alpha cells [24]. The state model approach for channel kinetics could highlight information about the main independent variables controlling channel gating [25]. This is particularly interesting in relation to alpha cells, as it could explain how electrical activity is related to glucagon release, and how channel functioning could affect glucose regulation. In agreement with the experimental observations we have considered that channel activation and deactivation are functions of the membrane voltage. Moreover, we have fixed deactivation parameters for fast changing currents (I_{Ca_N}, I_{Ca_T}, I_{Na}, and I_{K_A}), to efficiently estimate model parameters. These constraints helped to improve model identifiability [22]. For channel inactivation, we have assumed that channels inactivate in a sigmoidal manner, considering the half-inactivation voltage values reported in alpha cell experiments. For N-type calcium channels, we also found it necessary to include a dependence on external and internal calcium concentrations to correctly simulate inactivation. This fact links N- calcium current to a main role in calcium influx and calcium homeostasis. This is interesting since this influx may trigger glucagon release, as discussed in [24, 14].

Another topic emerging from our analysis are whole-cell conductances and channel populations in alpha cells. Whole-cell conductances are estimated as the maximal number of open channels multiplied by the unitary conductance. Although the unitary conductance is an intrinsic channel property, the maximal conductance depends on the cell type since it is a function of total channel population and opening probability. Based on our estimations, maximal whole-cell conductances for an alpha cell seem to be graded as follows: $g_{Na} \simeq g_K \gg g_{Ca}$, where each ion conductance g_x is calculated as the product of the estimated channel population and the unitary conductance, and $g_{Ca} = g_{Ca_T} + g_{Ca_N}$ and $g_K = g_{K_A} + g_{K_{DR}}$ (see Table 3). Our whole-cell conductance values highly agree with those used in a modelling work for alpha cells based on the Hodgkin-Huxley approach [7]. Our channel densities are also in the same magnitude order than values found in chromaffin and beta cells and used by some modelling works [17, 21]. We emphasize that our estimated conductances indicate that alpha cells are highly permeable to sodium and potassium which mainly manage action potentials, depolarising and repolarising the cell respectively [24, 14].

Channel densities, as well as single-channel currents in alpha cells, are still not known. This is probably because these cells are scarce and it is difficult to isolate them [24]. To make a comparison, it has been reported that mouse pancreatic beta cells contain less than 500 L-type calcium channels which corresponds to a density of 0.9 per square micron [3]. It is well worth noticing that our estimated channel population for N-type calcium channels in alpha cells is in the same order, since we

have ~ 200, which would correspond to a density of 0.6 (see Table 3). This finding is strongly relevant since both, L-type and N-type calcium channels, play a main role in insulin and glucagon secretion, respectively [3, 24].

The present work attempts to bridge the gap between electrophysiological recordings and modeling related to glucagon secretion. Our final aim is to simulate the whole alpha-cell electrical activity observed during low-glucose periods, which involves all channel models working together; this complex simulation will be better understood keeping minimal models. These state models are able to simulate interesting experimental conditions, such as channel knocking or specific therapeutic inhibitions through changes in channel properties. Another interesting goal for the future is to model zinc influence on the alpha-cell electrical activity. This is relevant since it has been proposed that zinc ions, co-secreted with insulin from neighbouring beta cells, might be involved in the suppression of glucagon secretion [29]. This suppressive effect depends on the action of zinc on alpha-cell K_{ATP} channels, opening them and inducing membrane potential hyperpolarization, which leads to the inhibition of glucagon secretion.

In order to study the electrical activity related to glucagon secretion following physiological protocols, the state modeling approach is adequate because these models are suitable to be used in microscopic simulations. These kind of simulations allow to understand secretion in exocytotic zones as well as the role of channel clustering, buffered Ca^{2+} diffusion and Ca^{2+} triggering in release. All of them are useful tools when studying exocytotic dynamics, as demonstrated in other neuroendocrine cells like adrenal chromaffin cells [26] and pancreatic beta cells [3].

Acknowledgments. The authors acknowledge financial support from I-MATH (Project C3-0136) and the Ministerio de Ciencia e Innovación (BFU 2007-67607), Spain. V. González-Vélez thanks CONACyT-México for her PhD scholarship. We would also like to thank the reviewers for their valuable comments and suggestions.

REFERENCES

[1] G. C. Amberg, S. D. Koh, Y. Imaizumi, S. Ohya and K. M. Sanders, *A-type potassium currents in smooth muscle*, Am. J. Physiol. Cell Physiol., **284** (2003), 583–595.

[2] S. Barg, J. Galvanovskis, S. O. Göpel, P. Rorsman and L. Eliasson, *Tight coupling between electrical activity and exocytosis in mouse glucagon-secreting α-cells*, Diabetes, **49** (2000), 1500–1510.

[3] S. Barg, X. Ma, L. Eliasson, et al., *Fast exocytosis with few ca channels in insulin-secreting mouse pancreatic b cells*, Biophys. J., **81** (2001), 3308–3323.

[4] K. C. Bittner and D. A. Hanck, *The relationship between single-channel and whole-cell conductance in the t-type* ca^{2+} *channel* $ca_v3.1$, Biophys. J., **95** (2008), 931–941.

[5] M. Brissova, M. J. Fowler, W. E. Nicholson, A. Chu, B. Hirshberg, D. M. Harlan and A. C. Powers, *Assessment of human pancreatic islet architecture and composition by laser scanning confocal microscopy*, J. Histochem. Cytochem., **53** (2005), 1087–1097.

[6] R. C. Cannon and G. D'Alessandro, *The ion channel inverse problem: Neuroinformatics meets biophysics*, PLoS Computational Biology, **2** (2006), 862–869.

[7] P. M. Diderichsen and S. O. Göpel, *Modelling the electrical activity of pancreatic α-cells based on experimental data from intact mouse islets*, J. Biol. Phys., **32** (2006), 209–229.

[8] C. P. Fall, E. S. Marland, J. M. Wagner and J. J. Tyson, "Computational Cell Biology," 1^{st} ed., Springer-Verlag, New York, 2002.

[9] Z.-P. Feng, J. Hamid, C. Doering, S. E. Jarvis, G. M. Bosey, E. Bourinet, T. P. Snutch and G. W. Zamponi, *Amino acid residues outside of the pore region contribute to n-type calcium channel permeation*, J. Biol. Chem., **276** (2001), 5726–5730.

[10] A. Gil and V. González-Vélez, *Exocytotic dynamics and calcium cooperativity effects in the calyx of held synapse: A modelling study*, J. Comput. Neurosci., **28** (2010), 65–76.

[11] V. González-Vélez and H. González-Vélez, *Parallel stochastic simulation of macroscopic calcium currents*, J. Bioinf. Comput. Biol., **5** (2007), 755–772.
[12] S. O. Göpel, T. Kanno, S. Barg, X-G. Weng, J. Gromada and P. Rorsman, *Regulation of glucagon release in mouse α-cells by k_{ATP} channels and inactivation of ttx-sensitive na^+ channels*, J. Physiol., **528** (2000), 509–520.
[13] J. Gromada, K. Bokvist, W.-G. Ding, S. Barg, K. Buschard, E. Renström and P. Rorsman, *Adrenaline stimulates glucagon secretion in pancreatic a-cells by increasing the ca^{2+} current and the number of granules close to the l-type ca^{2+} channels*, J. Gen. Physiol., **110** (1997), 217–228.
[14] J. Gromada, I. Franklin and C. B. Wollheim, *alpha-cells of the endocrine pancreas: 35 years of research but the enigma remains*, Endocrine Rev. **28** (2007), 84–116.
[15] M. Gurkiewicz and A. Korngreen, *A numerical approach to ion channel modelling using whole-cell voltage-clamp recordings and a genetic algorithm*, PLoS Computational Biology, **3** (2007), 1633–1647.
[16] H. Kasai and E. Neher, *Dihydropyridine-sensitive and omega-conotoxin-sensitive calcium channels in a mammalian neuroblastoma-glioma cell line*, J. Physiol., **448** (1992), 161–188.
[17] J. Klingauf and E. Neher, *Modeling buffered ca^{2+} diffusion near the membrane: Implications for secretion in neuroendocrine cells*, Biophys. J., **72** (1997), 674–690.
[18] Y. M. Leung, I. Ahmed, L. Sheu, R. G. Tsushima, N. E. Diamant and H. Y. Gaisano, *Two populations of pancreatic islet α-cells displaying distinct ca^{2+} channel properties*, Biochem. Biophys. Res. Comm., **345** (2006), 340–344.
[19] Y. M. Leung, I. Ahmed, L. Sheu, R. G. Tsushima, N. E. Diamant, M. Hara and H. Y. Gaisano, *Electrophysiological characterization of pancreatic islet cells in the mouse insulin promoter-green fluorescent protein mouse*, Endocrinology, **146** (2005), 4766–4775.
[20] P. E. MacDonald, Y. Z. De Marinis, R. Ramracheya, A. Salehi, X. Ma, P. R. V. Johnson, R. Cox, L. Eliasson and P. Rorsman, *A k_{ATP} channel-dependent pathway within α cells regulates glucagon release from both rodent and human islets of langerhans*, PLoS Biology, **5** (2007), 1236–1247.
[21] M. E. Meyer-Hermann, *The electrophysiology of the β-cell based on single transmembrane protein characteristics*, Biophys. J., **93** (2007), 2952–2968.
[22] L. S. Milescu, G. Akk and F. Sachs, *Maximum likelihood estimation of ion channel kinetics from macroscopic currents*, Biophys. J., **88** (2005), 2494–2515.
[23] F. Qin, *Principles of single-channel kinetic analysis*, Meth. Mol. Biol., **288** (2007), 253–286.
[24] I. Quesada, E. Tudurí, C. Ripoll and A. Nadal, *Physiology of the pancreatic α-cell and glucagon secretion: Role in glucose homeostasis and diabetes*, J. Endocrin., **199** (2008), 5–19.
[25] M. S. P. Sansom, F. G. Ball, C. J. Kerry, R. McGee, R. L. Ramsey and P. N. R. Usherwood, *Markov, fractal, diffusion, and related models of ion channel gating*, Biophys. J., **56** (1989), 1229–1243.
[26] J. Segura, A. Gil and B. Soria, *Modeling study of exocytosis in neuroendocrine cells: Influence of the geometrical parameters*, Biophys. J., **79** (2000), 1771–1786.
[27] J. R. Serrano, E. Pérez-Reyes and S. W. Jones, *State-dependent inactivation of the $\alpha 1g$ t-type calcium channel*, J. Gen. Physiol., **114** (1999), 185–201.
[28] M. F. Sheets, B. E. Scanley, D. A. Hanck, J. C. Makielski and H. A. Fozzard, *Open sodium channel properties of single canine cardiac purkinje cells*, Biophys. J., **52** (1987), 13–22.
[29] M. Slucca, J. S. Harmon, E. A. Oseid, J. Bryan and R. P. Robertson, *Atp-sensitive k^+ channel mediates the zinc switch-off signal for glucagon response during glucose deprivation*, Diabetes, **59** (2010), 128–134.
[30] D. O. Smith, J. L. Rosenheimer and R. E. Kalil, *Delayed rectifier and a-type potassium channels associated with k_v2.1 and k_v4.3 expression in embryonic rat neural progenitor cells*, PLoS One, **3** (2008), 1–9.
[31] A. F. Strassberg and L. J. DeFelice, *Limitations of the Hodgkin-Huxley formalism: Effects of single channel kinetics on transmembrane voltage dynamics*, Neural Comp., **5** (1993), 843–855.
[32] N. A. Tamarina, A. Kuznetsov, L. E. Fridlyand and L. H. Philipson, *Delayed-rectifier (k_v2.1) regulation of pancreatic β-cell calcium responses to glucose: Inhibitor specificity and modeling*, Am. J. Physiol. Endocrinol. Metab., **289** (2005), E578–E585.
[33] T. I. Tóth and V. Crunelli, *Estimation of the activation and kinetic properties of i_{Na} and i_k from the time course of the action potential*, J. Neurosci. Meth., **111** (2001), 111–126.

[34] E. Tudurí, E. Filiputti, E. M. Carneiro and I. Quesada, *Inhibition of ca^{2+} signaling and glucagon secretion in mouse pancreatic α-cells by extracellular atp and purinergic receptors*, Am. J. Physiol. Endocrinol. Metab., **294** (2008), E952–E960.

[35] C. A. Vandenberg and F. Bezanilla, *A sodium channel gating model based on single channel, macroscopic ionic, and gating currents in the squid giant axon*, Biophys. J., **60** (1991), 1511–1533.

[36] S. Vignali, V. Leiss, R. Karl, F. Hofmann and A. Welling, *Characterization of voltage-dependent sodium and calcium channels in mouse pancreatic a- and b-cells*, J. Physiol., **572** (2006), 691–706.

[37] J. Villanueva, C. J. Torregrosa-Hetland, A. Gil, V. González-Vélez, J. Segura, S. Viniegra and L. M. Gutiérrez, *The organization of the secretory machinery in neuroendocrine chromaffin cells as a major factor to model exocytosis*, HFSP Journal, **4** (2010), 85–92.

[38] S. Wang, V. E. Bondarenko, Y. Qu, M. J. Morales, R. L. Rasmusson and H. C. Strauss, *Activation properties of k_v4.3 channels: Time, voltage and $[k^+]_o$ dependence*, J. Physiol., **557** (2004), 705–717.

[39] A. R. Willms, *Neurofit: Software for fitting hodgkin-huxley models to voltage-clamp data*, J. Neurosci. Meth., **121** (2002), 139–150.

[40] A. R. Willms, D. J. Baro, R. M. Harris-Warrick and J. Guckenheimer, *An improved parameter estimation method for hodgkin-huxley models*, J. Comp. Neurosci., **6** (1999), 145–168.

[41] G. Zamponi, "Voltage-gated Calcium Channels," 1^{st} ed., Kluwer Academic/Plenum Publishers, New York, 2005.

Received April 9, 2010; Accepted August 16, 2010.

E-mail address: amparo.gil@unican.es
E-mail address: vgv@correo.azc.uam.mx
E-mail address: ivanq@umh.es